Journal of Hydrology 537 (2016) 367–381

Contents lists available at ScienceDirect

Journal of Hydrology

journal homepage: www.elsevier.com/locate/jhydrol

On the identification of representative *in situ* soil moisture monitoring stations for the validation of SMAP soil moisture products in Australia

Mei Sun Yee [a,*], Jeffrey P. Walker [a], Alessandra Monerris [a], Christoph Rüdiger [a], Thomas J. Jackson [b]

[a] *Department of Civil Engineering, Monash University, Clayton, Australia*
[b] *USDA-ARS Hydrology and Remote Sensing Laboratory, Beltsville, MD 20705-2350, USA*

ARTICLE INFO

Article history:
Received 12 August 2015
Received in revised form 29 February 2016
Accepted 26 March 2016
Available online 2 April 2016
This manuscript was handled by Andras Bardossy, Editor-in-Chief, with the assistance of Axel Bronstert, Associate Editor

Keywords:
Soil moisture measurement
Representativeness
Soil Moisture Active Passive (SMAP)
Satellite validation
Temporal stability
Spatial stability

SUMMARY

The high spatio-temporal variability of soil moisture complicates the validation of remotely sensed soil moisture products using *in situ* monitoring stations. Therefore, a standard methodology for selecting the most representative stations for the purpose of validating satellites and land surface models is essential. Based on temporal stability and geostatistical studies using long-term soil moisture records, intensive ground measurements and airborne soil moisture products, this study investigates the representativeness of soil moisture monitoring stations within the Yanco study area for the validation of NASA's Soil Moisture Active Passive (SMAP) products at 3 km for radar, 9 km for radar–radiometer and 36 km for radiometer pixels. This resulted in the identification of a number of representative stations according to the different scales. Although the temporal stability method was found to be suitable for identifying representative stations, stations based on the mean relative difference (MRD) were not necessarily the most representative of the areal average. Moreover, those identified from standard deviation of the relative difference (SDRD) may be dry-biased. It was also found that in the presence of heterogeneous land use, stations should be weighted based on proportions of agricultural land. Airborne soil moisture products were also shown to provide useful *a priori* information for identifying representative locations. Finally, recommendations are made regarding the design of future networks for satellite validation, and specifically the most representative stations for the Yanco area.

1. Introduction

Soil moisture plays a critical role in land surface–atmosphere interaction through the partitioning of available energy into sensible and latent heat fluxes (Entekhabi et al., 2010; Prigent et al., 2005), controlling the ratio of runoff to groundwater recharge (Delworth and Manabe, 1988), and feedback tendency with precipitation (Koster, 2004; Pal and Eltahir, 2003). Advances in remote sensing and the launch of dedicated soil moisture satellites such as the European Space Agency's (ESA) Soil Moisture and Ocean Salinity (SMOS) (Kerr et al., 2010) and the National Aeronautics and Space Administration's (NASA) Soil Moisture Active Passive (SMAP) (Entekhabi et al., 2010) provide a mechanism for estimating soil moisture at global scales, which is impossible using only field measurements (Refsgaard, 1997). These soil moisture products can be assimilated into models to improve flood, weather and climate forecasting, as well as irrigation and cropping practices (Brocca et al., 2012; de Wit and van Diepen, 2007; Engman, 1991; Koster, 2004; Koster et al., 2009; Walker et al., 2001).

Typically, satellite soil moisture products are validated against *in situ* measurements (Albergel et al., 2012; Choi et al., 2008; Draper et al., 2009; Jackson et al., 2010) or detailed airborne field campaigns (e.g. Bosch et al., 2006; Famiglietti et al., 1999; Jackson et al., 1999; McNairn et al., 2015; Peischl et al., 2012). While *in situ* measurements are the most accurate method for measuring soil moisture at a point, they may not be representative of a satellite footprint due to differences in spatial scale (point scale vs several kms of satellite footprint). To minimize errors attributed to upscaling point measurements to the satellite's footprint, measurements from several soil moisture stations can be averaged or interpolated, or a transfer function applied to upscale the soil moisture measurements, or a representative soil moisture station can be identified (Crow et al., 2012; De Lannoy et al., 2006). Interpolation of station measurements can be based on geostatistical methods such as block-kriging (e.g. Vinnikov et al., 1999) whereas land surface models or satellite observations of a finer resolution can be used to derive a transfer function for upscaling measurements from soil moisture stations (e.g. Crow et al., 2005; Qin et al., 2013).

Although efforts to increase long-term and large scale ground observations of soil moisture have been increasing (e.g. Dorigo

* Corresponding author.
E-mail address: mei.yee@monash.edu (M.S. Yee).

http://dx.doi.org/10.1016/j.jhydrol.2016.03.060
0022-1694/

et al., 2011; Robock et al., 2000), even the densest network is inadequate for the evaluation of coarse-resolution soil moisture products, typically covering only a fraction of a single footprint. Therefore, where long-term and large-scale measurements of soil moisture are available, it is important that these datasets be exploited to assess the quality of the soil moisture stations prior to application for validation purposes. Moreover, the resources required to maintain extensive monitoring networks can be demanding. As networks age and/or support for these monitoring networks wane, it is anticipated that resource demand to maintain these networks will increase. In spite of this, long-term records are still needed for long-term validation purposes. Consequently, the ability to identify a subset of stations which can provide the same information for validation purposes would be valuable (Bittelli, 2011; Crow et al., 2012; Gruber et al., 2013).

One of the ways in which representative stations can be identified is based on temporal, rank or order stability (You-Jun, 2006). Vachaud et al. (1985) observed that due to its soil properties, soil moisture values within a field do not vary much across long time scales at certain points with respect to the average soil moisture, whereas other points are consistently wetter (wet-biased) or drier (dry-biased) than the areal average. This concept has been applied in the past to identify representative locations for long-term validation of remotely sensed soil moisture products or model simulations (e.g. Cosh, 2004; De Lannoy et al., 2006; Gómez-Plaza et al., 2000; Jacobs et al., 2004; Li and Shao, 2015; Martínez-Fernández and Ceballos, 2005; Schneider et al., 2008; Zhou et al., 2015) as it can reduce the number of soil moisture monitoring stations needed to provide the same information for validation activities (Cosh et al., 2006). However, these studies assume that the average of measurements from all stations provide an accurate estimation of the areal average soil moisture.

In principle, a location which is able to demonstrate the ability to capture the mean of the field with a small bias (low mean relative difference: MRD) and low variability (i.e. low standard deviation of the relative difference: SDRD) would be a representative station (refer to Eqs. (1)–(4) in Section 4). However, this can be difficult to define and is dependent on the scale in question (Cosh, 2004). Previous studies have identified representative stations based on a MRD < 0.1 m^3/m^3 and a low SDRD (e.g. Schneider et al., 2008), or purely based on MRD or SDRD (e.g. Grayson and Western, 1998; Martínez-Fernández and Ceballos, 2003), or a combination of both (e.g. Jacobs et al., 2004). The index which combines both MRD and SDRD to overcome the limitations intrinsic to the use of MRD or SDRD on its own was first introduced by Jacobs et al. (2004) as root mean square error (RMSE) and later coined as index of time stability (ITS) by Zhao et al. (2010) to prevent confusion with the general definition of RMSE. Based on a simulation study, Martínez et al. (2014) showed that the performance indicators used for selecting representative locations was most consistent based on MRD whereas those based on SDRD changed depending on weather patterns and sampling patterns. Conversely, several authors including Hu et al. (2012) and Gao et al. (2013) have compared the use of different time stability indicators using *in situ* measurements and recommended using ITS (or RMSE). Following this, Penna et al. (2013) successfully identified representative locations for two hillslopes based on RMSE. However, as these studies were for scales ranging from 0.005 km^2 to 0.31 km^2, it would be valuable to compare them at larger scales, because even operational soil moisture products retrieved from the Sentinel-1 satellites acquiring SAR data in C-band, will be 1 km^2 (Wagner et al., 2009).

Since the identification of a time-stable location requires long-term *a posteriori* information, the ability to identify a time-stable location using *a priori* information is of more value as it eliminates the need for establishing extensive soil moisture networks (Gómez-Plaza et al., 2000; Grayson and Western, 1998; Zhao et al., 2010). Several studies have tried to relate soil, vegetation, topographic and land use features of time-stable locations to features which can be used as *a priori* information for identifying a time-stable location (e.g. De Lannoy et al., 2006; Jacobs et al., 2004; Mohanty and Skaggs, 2001; Zhao et al., 2010). Another method with potential is a slight modification of the regular variogram to characterize the spatial variability of soil moisture with respect to the stations (herein referred to as the centered-variogram). The centered-variogram represents the spatial variability of the variable under consideration radiating outwards from a point. It has previously been applied to determine the spatial representativeness of air-temperature records (Janis and Robeson, 2004) and tower albedo measurements (Román et al., 2009) but its potential to determine the spatial representativeness of soil moisture monitoring stations has not been explored. The possibility of using a centered-variogram to identify a representative station is attractive since it can possibly be used to identify representative points prior to setting up a soil moisture network based on observations from an airborne sensor.

The availability of a unique suite of data which includes intensive ground soil moisture measurements (250 m spacing), aircraft measurements (1 km) and long-term soil moisture stations (~5 years) measurements across scales ranging from local (3 km) up to regional (36 km), distinguishes it from other small area (e.g. Brocca et al., 2012; De Lannoy et al., 2006; Hu et al., 2012) or short term (e.g. Cosh, 2004; Cosh et al., 2006; Famiglietti et al., 2008; Martínez-Fernández and Ceballos, 2005) studies. Consequently, using the Yanco core calibration/validation site for SMAP as a case study, this paper compares a temporal stability analysis based on long-term soil moisture observations from the OzNet Monitoring Network (OzNet) with high resolution soil moisture measurements taken during three extensive field campaigns (SMAPEx 1–3, Panciera et al., 2014) and airborne soil moisture products derived for the area (Gao et al., 2013), to assess the representativeness of stations within OzNet and make recommendations on the design of future networks. As SMAP integrates measurements from an L-band radar and an L-band radiometer to provide (i) ~3 km high resolution (radar only), (ii) ~36 km low resolution (radiometer only) and (iii) ~9 km intermediate resolution (combined radar–radiometer) soil moisture products, the analysis was carried out at these different scales.

2. Study area

The *in situ* soil moisture data for this study were obtained from the Yanco site (34.561–35.170°S, 145.826–146.439°E), a 60 km × 60 km intensive study area within the Murrumbidgee River catchment in New South Wales, Australia (Fig. 1) and a subset of the wider OzNet soil moisture network (Smith et al., 2012). The Yanco area is generally flat with elevations ranging from 117 m to 150 m, and its soil types are predominantly clays, red brown earth, transitional red brown earth, sands over clay, and deep sands. The region has a mean daytime temperature that varies from 32.1 °C in January to 13.5 °C in July. Annual rainfall has a mean of 418.5 mm, mostly falling during winter and late autumn (Bureau of Meteorology station ID. 074037). There is no preferential rainfall pattern in this area.

This area has been extensively monitored for remote sensing research, with soil moisture monitoring stations for soil moisture at various depths. Moreover, a series of field experiments has been performed, contributing to the pre- and post-launch algorithm development of missions such as SMOS and SMAP; National Airborne Field Experiment 2006 (Merlin et al., 2008), Australian Airborne Cal/Val Experiments for SMOS (Peischl et al., 2012) and

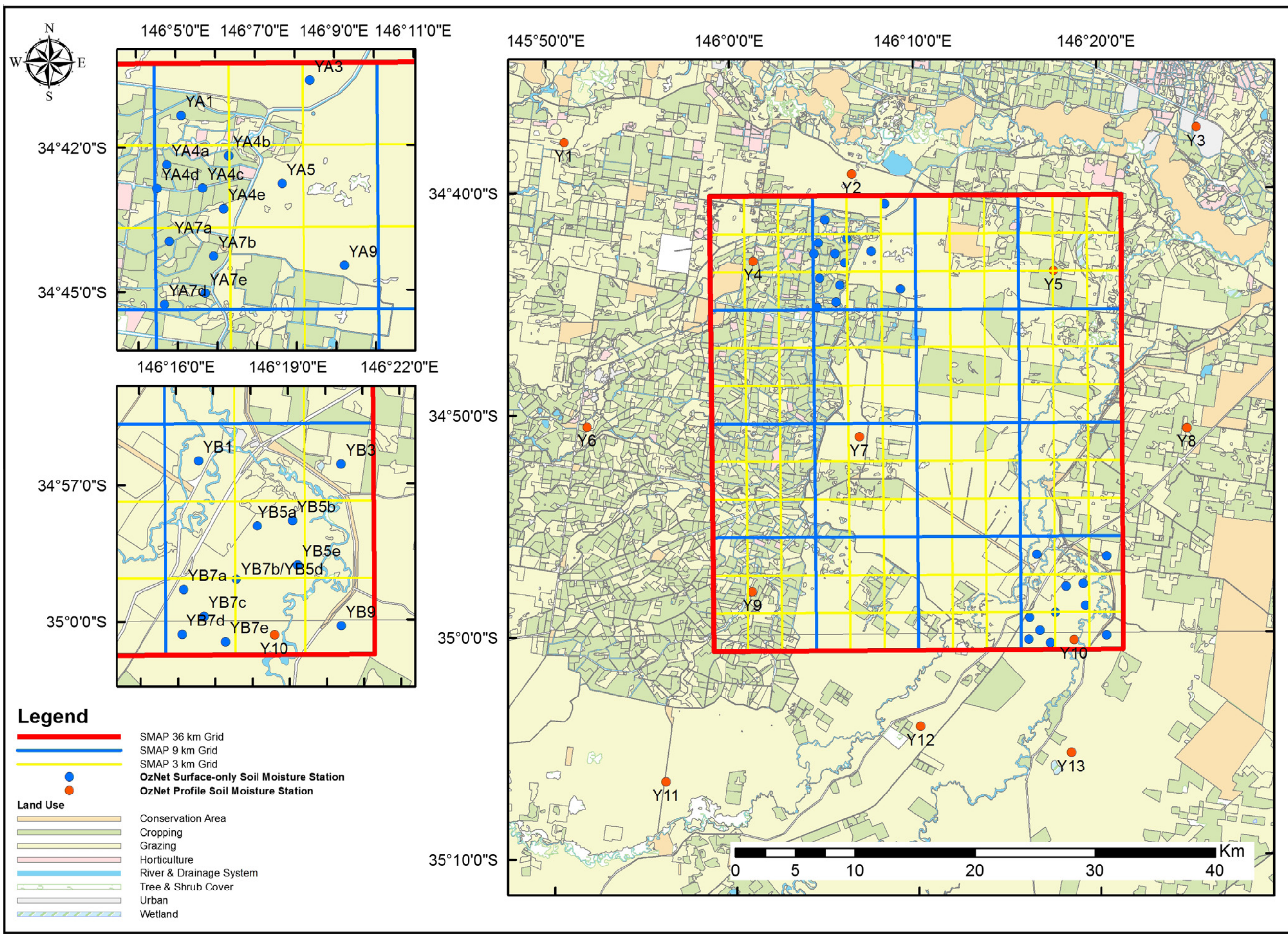

Fig. 1. Land use of study area overlaid with SMAP 3 km (yellow lines), 9 km (blue lines) and 36 km (red lines) pixels and locations of permanent Y-stations. Left insets show the distribution of the cluster YA- and within the 9 km pixels (top: YA, bottom: YB). (For interpretation of the references to color in this figure legend, the reader is referred to the web version of this article.)

Soil Moisture Active Passive Experiments (SMAPEx) (Panciera et al., 2014).

3. Data sets

To identify the representative stations, long-term soil moisture measurements from the OzNet soil moisture network, intensive measurements from a series of three airborne field experiments, SMAPEx-1 to -3, and 9 days of high-resolution soil moisture maps derived from airborne observations were used in this study (Table 1).

3.1. OzNet soil moisture monitoring network

The *in situ* soil moisture data of Yanco is part of the soil moisture monitoring network known as OzNet, which has been recording soil moisture data since 2001 (www.oznet.org.au, Smith et al., 2012). Within the study area, there are 13 sparsely distributed permanent stations (Y1–Y13), and two densely located clusters of stations (YA and YB) installed specifically for the SMAPEx field experiments (Fig. 1). This nomenclature is based on Smith et al. (2012) and Panciera et al. (2014).

Of the 13 permanent stations, 5 stations fall within one of the 36 km SMAP product pixels. These permanent stations were installed in 2003 and are equipped with a vertically installed Stevens Water Hydraprobe impedance sensors and Campbell Scientific CS616 frequency domain reflectometers to measure the soil moisture content at the sites, a Hydrological Services TB4 raingauge and a thermistor at 2.5 cm and 15 cm for soil temperature observations. The cluster stations only measure surface soil moisture using a Hydraprobe inserted vertically from the surface and soil temperature using Unidata 6507A temperature sensors at 1 cm, 2.5 cm and 5 cm. These cluster stations are concentrated within the YA and YB areas, which correspond to two nominal 9 km SMAP validation grid pixels (Fig. 1). The YA area is largely located within the Coleambally Irrigation Area (CIA) which consists of farms with a mix of flood irrigation and dryland cropping, whereas the YB area mainly consists of pastures for grazing. These cluster stations were installed in 2009–2010 with site locations selected in such a way that 4–5 stations would fall within each of two 3 km × 3 km focus areas for each of the 9 km areas (YA4 and YA7 within the YA area, and YB5 and YB7 within the YB area), thus corresponding to four nominal 3 km SMAP high resolution product pixels.

To differentiate the stations, permanent stations with profile measurements are denoted with the prefix ‘Y-’ whereas cluster stations with are denoted ‘YA-’ and ‘YB-’, and stations further concentrated within the 3 km pixels are denoted with ‘YA4-’, ‘YA7-’, ‘YB5-’ and ‘YB7-’ (Table 1). Half hourly surface soil moisture measurements (top 5 cm) from the period 1st December 2009 to 28th February 2015 were used in this study.

Table 1
Datasets used in study. Notation *i*, *x* and *y* indicates the number or alpha character used to differentiate stations within different SMAP grids. HDAS: Hydraprobe Data Acquisition System. PLMR: Polarimetric L-band Multibeam Radiometer. SMAP: Soil Moisture Active Passive.

Stations		SMAP reference grid (km)	Type	Resolution	Period
Permanent:	Y*i*; *i* = 1:13	Yanco	Point	–	Dec 2009–Feb 2015
Clusters:	YA*x*; *x* = 1, 3, 5, 9	9	Point	–	Dec 2009–Feb 2015
	YB*x*; *x* = 1, 3, 9	9			
	YA4*y*; *y* = a, b, c, d, e	3			
	YA7*y*; *y* = a, b, d, e	3			
	YB5*y*; *y* = a, b, d, e	3			
	YB7*y*; *y* = a, b, c, d, e	3			
PLMR		36	Average	1 km	9 days (SMAPEx-3)
HDAS (intensive)		3	3 samples per point	250 m	SMAPex-1 to -3

3.2. SMAPEx field campaigns

The Soil Moisture Active Passive Experiments (SMAPEx-1 to -3), aimed at the development and validation of SMAP high resolution soil moisture products, were carried out at the site from 2010 to 2011. SMAPEx-1 (Austral winter, 5–10 July 2010) and SMAPEx-2 (Austral summer, 4–8 December 2010) were conducted over a single week, whereas SMAPEx-3 (Austral spring, 5–23 September 2011) was performed across three weeks. More details regarding these campaigns including the experimental plan and site conditions can be found in Panciera et al. (2014).

During these campaigns, intensive ground sampling of soil moisture was carried out within the 3 km YA- and YB-pixels at a 250 m spacing (Table 1). Measurements from 0 to 5 cm were acquired using the Hydraprobe Data Acquisition System (HDAS), a spatial data acquisition tool which integrates a Hydraprobe and a hand-held PC with GPS (Merlin et al., 2008). Three measurements were taken within a radius of 1 m at each sampling location and these values averaged during post-processing. The calibration approach applied to the station and HDAS measurements were as described in Merlin et al. (2007) and verified using gravimetric samples. Due to heavy rainfall prior to SMAPEx-2, some areas were flooded meaning soil moisture observations were not available in the YB7 area.

3.3. Airborne soil moisture product

This study uses passive microwave data derived from regional flights during SMAPEx-3, prior to the launch of SMAP. The regional flights covered an area which coincided with the single SMAP 36 km radiometer pixel in Fig. 1. On-board the aircraft was the Polarimetric L-band Multibeam Radiometer (PLMR; 1413 MHz and bandwidth of 24 MHz, V-H polarization) installed in a push-broom configuration; meaning that the six beams are arranged across the flight path to enable a larger coverage of the area, and with a footprint resolution of approximately 1 km at 3 km flying altitude. The L-band brightness temperature data translates into 0–5 cm observation depth (Jackson et al., 1984). The brightness temperature was then used with parameters such as vegetation water content (VWC), soil surface roughness and soil temperature to derive an airborne soil moisture product at 1 km resolution using a τ–ω radiative transfer model (Y. Gao, personal communication, March 17, 2015). Rainfall events occurred from the 5th to the 7th (~5 mm) and 10th to 12th of September 2011 (~3 mm).

4. Methodology

A representative station is defined in this study as a station which measures soil moisture content close to the areal average of the SMAP pixel of interest, or one that can be used to obtain the average over an extended period (Vanderlinden et al., 2012). To do so, the representativeness of the stations in Fig. 1 were evaluated based on temporal stability analysis, comparisons between station measurements and high density roving measurements (point to pixel comparison), and geostatistical analysis (variogram and centered-variogram analysis) based on both high intensity ground measurements and 1 km airborne soil moisture product.

4.1. Temporal stability analysis

As temporal stability is well-documented in previous studies (e.g. De Lannoy et al., 2006; Gómez-Plaza et al., 2000; Martínez-Fernández and Ceballos, 2003), its theory will not be repeated here. The data record used in these previous studies have ranged from less than 1 year to 3 years; compared to the 5 years and 3 months of data here. Temporal stability analyses were performed here for (1) four 3 km pixels (YA4, YA7, YB5 and YB7); (2) two 9 km pixels (YA and YB); and (3) a single nominal SMAP 36 km pixel. Only the representative stations from the 3 km pixels were used in the subsequent analysis at 9 km, and likewise, only the most representative stations of the 9 km pixels were used for the 36 km pixel. The rationale for this was to avoid biasing the spatial mean from having more soil moisture stations in a certain area. Similarly, stations were only considered when at least 75% of the monitoring station's data were available. In addition, measurements which fell outside a station's 90% confidence interval over the entire study period were discarded to remove extreme outliers (Rüdiger et al., 2009). This resulted in the removal of more than 50% of the available dataset. From the analysis, MRD and SDRD were derived for each station. The areal mean soil moisture at time j for N stations is

$$\overline{\theta_j} = \frac{1}{N}\sum_{s=1}^{N}\theta_{s,j}, \tag{1}$$

where $\theta_{s,j}$ represents soil moisture observed by the sth station and jth time step, respectively. Therefore, the relative difference, RD, for station s at time j can be expressed as

$$\mathrm{RD}_{s,j} = \frac{\theta_{s,j} - \overline{\theta_j}}{\overline{\theta_j}}, \tag{2}$$

which gives MRD as

$$\mathrm{MRD}_s = \frac{1}{m}\sum_{j=1}^{m}\mathrm{RD}_{s,j}, \tag{3}$$

and SDRD as

$$\mathrm{SDRD}_s = \sqrt{\frac{1}{m-1}\sum_{j=1}^{m}(\mathrm{RD}_{s,j} - \mathrm{MRD}_s)^2}. \tag{4}$$

A station which measures soil moisture close to the spatial mean would have an MRD close to 0. At the same time, a low SDRD (time or rank stable) indicates that the station has a similar temporal pattern as the spatial mean soil moisture (De Lannoy et al., 2006). Ideally, a representative station would have a MRD and SDRD which is close to 0. It is noteworthy that temporally stable sites having a non-zero MRD can be used to represent the areal average soil moisture if the offset between the site and the areal average soil moisture is known (Grayson and Western, 1998). However, the assumption based on this method is that the offset is constant regardless of time and this has been questioned by previous studies (Gao et al., 2013; Heathman et al., 2012). Following Jacobs et al. (2004), to combine both MRD and SDRD, the root mean square error (RMSE) of the biases (MRD) and its precision (SDRD) was computed as

$$\mathrm{RMSE}_s = \sqrt{\mathrm{MRD}_s^2 + \mathrm{SDRD}_s^2}, \tag{5}$$

where s is the soil moisture station to account for both MRD and SDRD. For the remainder of this paper, the subscript s will be removed for MRD and SDRD as it should be understood that MRD and SDRD are station specific. However, to avoid confusion with RMSE used in statistics as a measure of the differences between values, RMSE_s will be retained to describe the RMSE of the RD. Note that MRD is a ratio and therefore is unitless.

In this study, a representative station is considered to be one with the lowest RMSE_s. However, as discussed previously, different studies have used different performance indicators to define representative stations. Therefore, to examine how different performance indicators can affect the results, the analysis was also carried out based on MRD (stations with MRD closest to zero) and SDRD (stations with SDRD closest to zero, i.e. time or rank stable) alone. Unless specified, the representative stations described in this paper are based on using RMSE_s as an indicator. Moving from a smaller (9 km) to a larger scale (36 km), it is assumed that the single stations within 9 km pixels without intensive sampling are also representative of the field scale. Subsequently, temporal stability analysis and point-to-pixel comparisons were conducted to identify the most representative stations within the 36 km pixel. This analysis was also extended beyond the 36 km SMAP pixel perimeter to include the nearby permanent (Y) stations.

4.2. Point to pixel comparison

Representative stations are identified above using the temporal stability method based on a set of stations. However, due to the low density of stations within each pixel, it is unclear whether those individual stations are actually representative of the soil moisture conditions at the local scale. Therefore, to investigate a station's representativeness locally, comparisons were made between daily averages for each station and intensive sampling performed on the same day. Similarly, using the airborne soil moisture product, the average soil moisture for the 36 km pixel was compared with the daily mean soil moisture for each station on the day the flight was made. Stations with the lowest mean bias compared to the average of all intensive measurements were considered as the most representative of the areal average. Bias here was computed as

$$\mathrm{Bias} = |(\overline{\theta_A} - \overline{\theta_B})|, \tag{6}$$

where $\overline{\theta_A}$ is the spatial mean from sample A and $\overline{\theta_B}$ is the spatial mean from sample B.

4.3. Centered-variogram

To characterize the spatial distribution of soil moisture within the SMAP product, omni-directional variograms (herein referred to as standard variograms) for each pixel were derived in the same manner as previous studies (e.g. De Lannoy et al., 2006; Joshi and Mohanty, 2010; Western et al., 1998). The experimental variogram of soil moisture pairs at separation distance h, is then given by

$$\gamma(h) = \frac{1}{2n(h)} \sum_{i,j} (\theta_i - \theta_j)^2, \tag{7}$$

where $n(h)$ is the number of pairs of observations at separation distance h, θ_i and θ_j are soil moisture values at i and j. These experimental variograms were then fitted with the Whittle's elementary correlation function (Whittle, 1954) (herein referred to as the Whittle function). Although previous studies have applied the exponential model (e.g. De Lannoy et al., 2006; Western et al., 1998), by comparing several variogram models, the Whittle function was found to perform the best in this case based on goodness of fit statistics. The Whittle function is given by

$$\gamma(h) = c_0 + c\left[1 - \frac{h}{r} K_1\left(\frac{h}{r}\right)\right], \tag{8}$$

where c is the sill, c_0 is the nugget, r is the distance parameter and K_1 is the modified Bessel function of the second kind. The effective range of the Whittle function is defined as the distance when the variance reaches 95% of the sill, which is approximately equivalent to $4r$. A least squares minimization of the error between the Whittle function and the experimental variogram was performed to derive c, c_0 and r. The standard variogram was derived using intensive ground measurements for each 3 km pixel during each campaign (one per week) and using the 9 days of airborne soil moisture over a 36 km pixel to characterize the spatial variability of soil moisture within these pixels.

The point-centered-variogram was fashioned similarly to the standard variogram in Eq. (7) with a modification such that

$$\gamma(h) = \frac{1}{2n(h)} \sum_{i,s} (\theta_i - \theta_s)^2, \tag{9}$$

where θ_s is the daily average soil moisture of the stations and θ_i is the intensive soil moisture (ground or airborne) measured at distance h from the station. Each experimental centered-variogram was fitted with the Whittle function to derive c, c_0 and r as with the standard variograms. However, unlike the standard variograms, centered-variograms are limited in the number of inter-station pairs. As the field campaigns were designed for the validation of airborne soil moisture products rather than representativeness of stations, biases caused by lack of data were expected for stations close to the edge of the sampling grid. Therefore, the results from the centered-variogram analysis conducted here are more applicable to recommending how future airborne campaigns for soil moisture monitoring networks could be designed in order to identify representative stations.

As the nugget, sill and range derived from each variogram change with mean soil moisture conditions, and are therefore spatially varying, the spatial representativeness was evaluated based on the ability of each station to resolve the coherent spatial variability across each pixel size. The hypothesis is that if the model derived based on fitting the Whittle function to a station's centered-variogram fits well with that of the standard variogram derived for the pixel under consideration, the station is representative of that pixel. The goodness of fit between the centered-variogram and standard variogram was based on the coefficient of determination, R^2, and RMSE between the two fitted variogram models. This analysis was carried out using the intensive ground measurements at 250 m spacing for the 3 km pixels, and with 1 km resolution airborne soil moisture for evaluation at the 36 km pixel.

5. Results and discussion

5.1. Temporal stability analysis

Stations derived from temporal stability analysis using long-term soil moisture measurements were ranked from the smallest to the largest MRD, with error bars indicating the SDRD (Fig. 2). The $RMSE_s$ for each station is indicated by the shaded bars. The position of the station within the graph indicates whether the station systematically underestimates (negative MRD) or overestimates (positive MRD) the areal average soil moisture. SDRD indicates the rank stability, whereby a low SDRD indicates a time or rank stable locations. As $RMSE_s$ takes into account both the MRD and SDRD, a station with a low $RMSE_s$ would have a near zero MRD and a small SDRD. Results based on different indicators (solely based on MRD, SDRD or $RMSE_s$) are summarized in Table 2.

Average MRD within the YA4 (0.20) 3 km pixel was the highest followed by YA7 (0.16), and YB5 and YB7 (both 0.12). The larger RD between stations and the areal average soil moisture within YA4 and YA7 may be attributed to the presence of mixed irrigation and cropping activities, as opposed to the YB areas which are mainly semi-arid grassland. Consequently, the average SDRD was the also the highest for YA4, followed by YA7, YB5 and YB7 (YA4: 0.47, YA7:0.35; YB5: 0.27, YB7: 0.24). Except for the YB5 area, representative stations identified from the different indicators, MRD, SDRD or $RMSE_s$, differed (Table 2). This suggests that the indicator used to select the most representative station may affect the results.

For the 9 km pixels, the non-representative stations at the 3 km scale were discarded and the analysis repeated with the additional stations. Fig. 2 shows results from temporal stability analysis after retaining representative stations based on $RMSE_s$. This time, YA5 and YB7a were found to be the most representative based on $RMSE_s$. Brocca et al. (2012), Vanderlinden et al. (2012) and Zhao et al. (2010) found that the range of MRD and/or SDRD increased with area due to the greater variability in soil type, vegetation cover and land use. A mixed result is observed here for the YA area (MRD: 0.12, SDRD: 0.32) and the YB area (MRD: 0.14, SDRD: 0.24). This may be an effect of selecting only the representative stations when moving from the 3 km to 9 km pixel. Fig. 3 shows the results of the temporal stability analysis if stations were not eliminated when moving from a smaller to larger pixel scale.

Comparing the average SDRD when all stations were included, the average MRD and the average SDRD was 0.21 and 0.43 for YA, and 0.13 and 0.29 for the YB 9 km pixel. The elimination of stations from one scale to another increased MRD and decreased SDRD for the YB area. On the other hand, both MRD and SDRD decreased for the YA 9 km pixel and is even lower than the average MRD and SDRD for the individual 3 km pixels. This is likely due to the higher concentration of cropping activities within YA4 and YA7 as seen in Fig. 1.

Nevertheless, stations which were found to be representative of the YA 9 km pixel were the same with or without eliminating stations (Table 2). However, for the YB 9 km pixel, the results differed. Based on MRD, YA1 and Y10 were found to be representative of the 9 km pixels (Table 2). In an earlier study, based on a shorter record of data, Disseldorp et al. (2013) also found that YA1 and Y10 were the most representative of the 9 km pixels based on MRD. In fact, despite the different datasets used, both studies found YA4b and YA7d to be most representative of YA4 and YA7 3 km pixels based on MRD. Results for the YB5 and YB7 area were slightly different, but this is due to the small MRD between sites within the YB5 and YB7 area. This shows that the stations are well-distributed within the 9 km pixels and gives a good estimate of the 9 km areal soil moisture.

For the 36 km pixel (Fig. 2), YA5 was found to be the most representative station based on $RMSE_s$ and Y7 based on MRD, whereas YA5d/YB7b was found to be representative based on SDRD. By including all other stations beyond the 36 km pixel (Yanco), although the range of MRD and SDRD increased (Fig. 2), results remained the same based on $RMSE_s$ and SDRD. Similarly, comparing with results based on not eliminating stations, a closer inspection of Fig. 3 reveal that YA5 and YB7a had the lowest $RMSE_s$ after YB7c for the 9 km, 36 km and wider Yanco area. As for the 9 km pixels, stations within each pixel scale are likely to be sufficiently well-distributed to be able to give a representative measurement of soil moisture for their respective grid. As a result, whether stations are eliminated or not when moving from one scale to another does not affect the results of the analysis. In the same way, a smaller subset of stations can be used to provide the same information for this study area.

Fig. 4 shows the time-series of average near-surface soil moisture during SMAPEx-3 (top) and between January 2013 to December 2014 (bottom) based on measurements from all stations without elimination (green), stations within the 36 km pixel (cyan), and stations within the entire Yanco area (yellow) after eliminating non-representative stations within the 3 km and 9 km pixels based on $RMSE_s$. Generally, the temporal dynamics of the three combinations agree with one another. As seen previously, this also indicates that the sites within OzNet is able to capture the rainfall events. In contrast to the 3 km and 9 km pixel, at 36 km pixels, rainfall is likely to be more influential in controlling the spatial variability of soil moisture than soil type, vegetation cover and land use at the event scale. Therefore, at 36 km scale, a few stations are adequate for estimating the areal average soil moisture providing they are representative (Brocca et al., 2012).

Although YB7c (light blue[1]) follows a similar pattern with that of the average of all stations, its peaks after a precipitation event are lower in magnitude compared to the average of all stations, thereby making it more temporally stable (small SDRD) in comparison to other stations. Drier sites have previously been found to be more time-stable (Hu et al., 2012; Martínez et al., 2014). In the same way, YB7c which is drier after precipitation events will also have a smaller SDRD and therefore smaller $RMSE_s$. As a result, choosing a representative station based on time or rank stability would favor drier stations when SDRD or $RMSE_s$ is used as an indicator. If YB7c were to be used for the validation of remote sensing soil moisture products, the products will appear to overestimate after a precipitation event.

In addition, the YB area is likely to have low SDRD values due to its location in a land used mainly for grazing activities. Conversely, where mixed land use is present, such as within the YA areas, both the spatial variation of soil moisture is also expected to differ from season to season depending on decisions made by farmers, which are difficult to forecast or predict. This leads to high MRD and SDRD of stations within the YA area. For the purpose of measuring the temporal dynamics of an area it has been suggested by Schneider et al. (2008) that temporal stability may be adequate; however, if the objective is to validate satellite products, the ability of a station to represent the spatial mean of the satellite product pixel is more important. A station which is located within an area where mixed land use is present will unlikely be temporally stable. But, this does not mean that it is unrepresentative or that it cannot provide any information regarding the spatial variability of soil moisture. This is further investigated in the next section.

[1] For interpretation of color in Figs. 1 and 9, the reader is referred to the web version of this article.

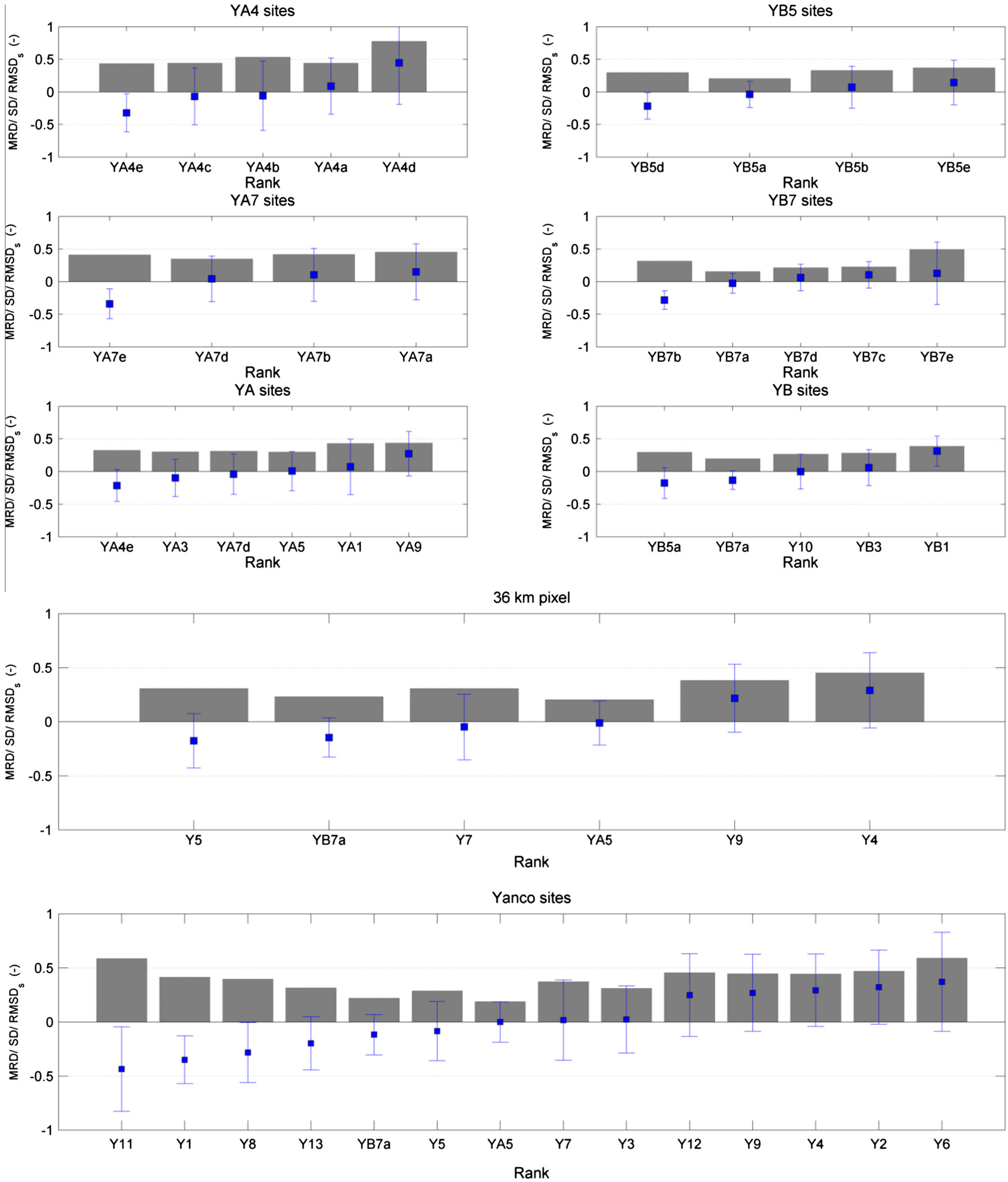

Fig. 2. Rank-ordered MRD for stations within YA4, YA7, YB5 and YB7 3 km pixels; YA and YB 9 km pixels, the 36 km SMAP pixel and the Yanco study area. Squares: Mean relative difference, MRD; Error bars: Standard deviation of MRD, ±SDRD; Shaded bars: Root mean square error of MRD and SDRD, $RMSE_s$.

5.2. Point to pixel

In this analysis, intensive ground sampling taken across the four 3 km SMAP pixels was divided into 1 km pixels to enable comparisons between stations at 1 km and 3 km scales. Intensive soil moisture measurements were found to be wetter compared to stations for the YA7 (0.12 m^3/m^3), YB5 (0.06 m^3/m^3) and YB7 (0.05 m^3/m^3) areas (Fig. 5). This may be caused by the establishment of the station itself and/or selection of the location of the station (which in YB was largely along the fence line). Moreover, the daily variation of soil moisture for each station was largest during SMAPEx-2 (Fig. 5) for all stations due to a dry-down event

Table 2
Representative stations based on different methods for each pixel and recommendations for long-term validation.

Pixel	Focus area	Method of identification					Rep.[a] station
		Temporal stability[b]			Point to pixel[c]	Centered variogram[c]	
		MRD	SD	$RMSE_s$	MRD	Best fit	
3 km	YA4	YA4b	YA4e	YA4e	YA4b	YA4e	YA4b/Weight[d]
	YA7	YA7d	YA7e	YA7d	YA7b	YA7e	YA7b/Weight[d]
	YB5	YB5a	YB5a	YB5a	YB5e	YB5d	YB5e
	YB7	YB7a	YB7b	YB7a	YB7e	YB7a	YB7e
9 km	YA	YA1 (YA1)	YA7e (YA7e)	YA5 (YA5)	–	–	YA5
	YB	Y10 (YB7d)	YB7b (YB7a)	YB7a (YB7c)	–	–	YB7a
36 km	Y	Y7 (YA4c)	YB5d/YB7b (YB5d/YB7b)	YA5 (YB7c)	YB7e, YA5	YB3	YA5
Yanco	Y	Y3 (YA4c)	YB5d/YB7b (YB5d/YB7b)	YA5 (YB7c)	YB7e, YA5	YB3	YA5

[a] Representative.
[b] Based entirely on stations. Stations in brackets are representative stations when analysis was carried out without eliminating stations from one pixel scale to another.
[c] Based on intensive ground samples for 3 km pixel and airborne soil moisture for 36 km and Yanco pixel.
[d] Weighted average of different stations based on landuse area occupied by the station.

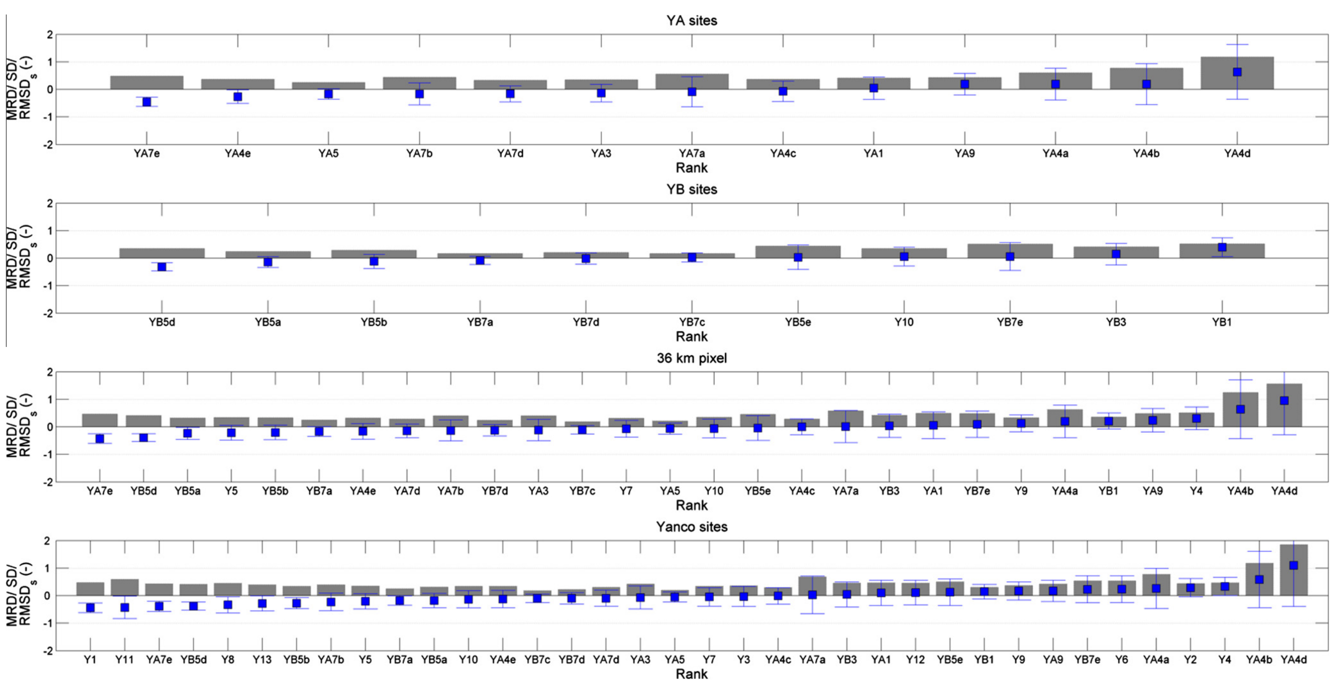

Fig. 3. Rank-ordered MRD for stations within the 36 km SMAP pixel and the Yanco study area without elimination of stations from one scale to another. Squares: Mean relative difference, MRD; Error bars: Standard deviation of MRD, ±SDRD; Shaded bars: Root mean square error of MRD and SDRD, $RMSE_s$. YB5d and YB7b are the same station but is indicated as YB5d here due to space limitation.

after extreme rainfall which fell before the campaign and on the last day of the campaign (53 mm between November 1 and December 1).

Some stations located in cropping areas also registered an increase of soil moisture due to flooding irrigation. For example, YA7a was also found to be almost 0.30 m^3/m^3 higher than the closest intensive sample during SMAPEx-2, but during SMAPEx-1, it was 0.10 m^3/m^3 lower (Fig. 5). The data for these periods were not removed from the analysis, as by doing so the spatial average soil moisture would appear lower. In the case of temporal stability, when a station shows a behavior which is different from that of other stations, it would be penalized and therefore, deemed to be unrepresentative (as seen from the previous section). However, in terms of spatial average, it is actually representing the irrigated or flooded areas of the pixel.

For 1 km pixels, the spatial variation within each pixel was larger than the daily variation measured at the stations, at times up to 0.20 m^3/m^3 (Fig. 6). Generally, the spatial variation within a pixel was the highest for YA4 followed by YA7, YB5 and the lowest for YB7, as expected due to the presence of agricultural and cropping activities in the YA areas. During SMAPEx-1 and SMAPEx-2, soil moisture from intensive sampling were generally found to be wetter than the station measurements (YA4: 0.06 m^3/m^3; YA7: 0.07 m^3/m^3; YB5: 0.05 m^3/m^3; YB7: 0.06 m^3/m^3). Compared to Fig. 5, by taking an average of station measurements within the 1 km pixel, the majority of points from intensive measurements at YA7 moved closer to the 1:1 line, as the uncertainty in each measurement decreased with more measurements. For the YB5 and YB7 pixels, little change is observed between Figs. 5 and 6. This is likely due to the relative homogeneity of both soil properties and land use within the YB area.

In the case of 3 km pixels, while some individual stations seem to perform better whereas others performed worse, stations that performed well generally did so for all campaigns (e.g. YA7b). Nevertheless, YA4b, YA7b and YB5e were identified as the representative stations of their respective 3 km pixels based on point

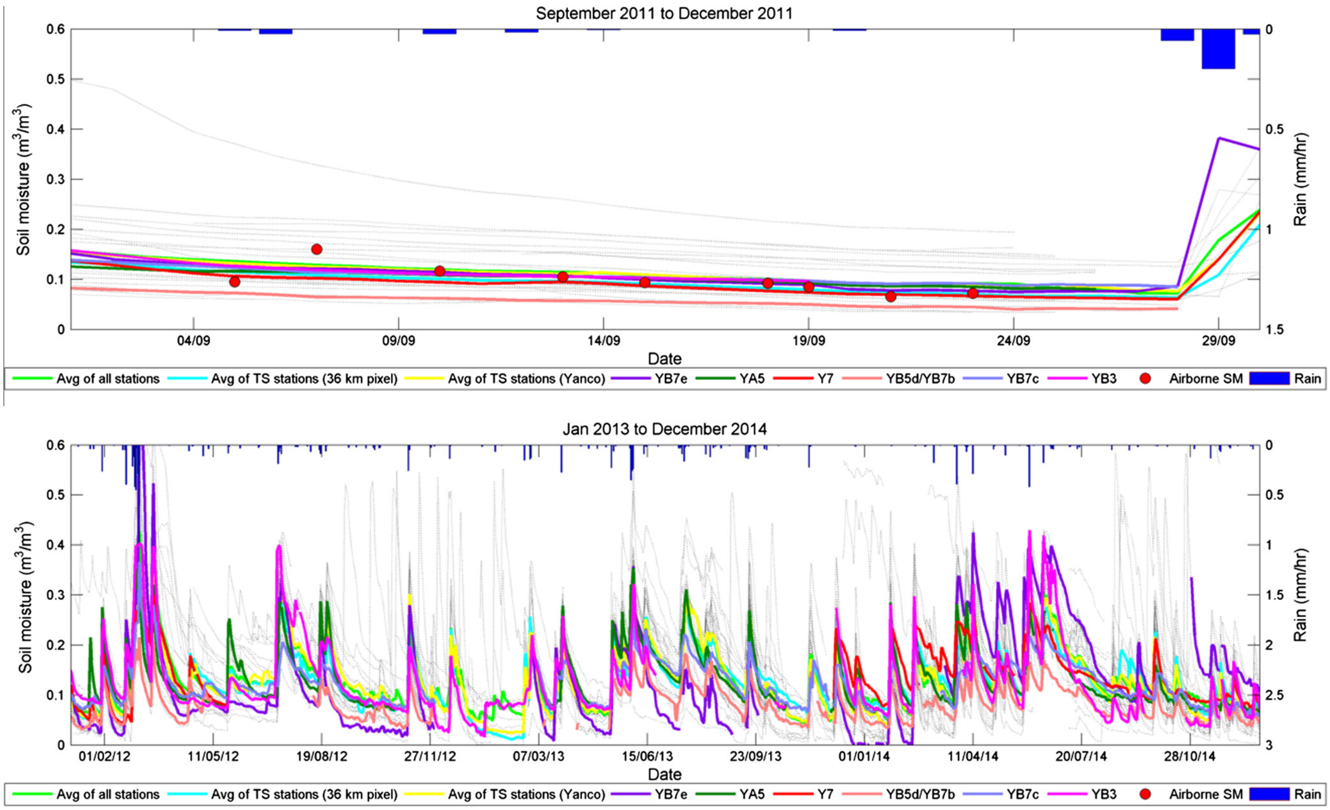

Fig. 4. Timeseries of near-surface (0–5 cm) soil moisture measurements comparing different representative soil moisture stations at 36 km scales identified based on different methods. The gray lines are measurements from stations which were not selected.

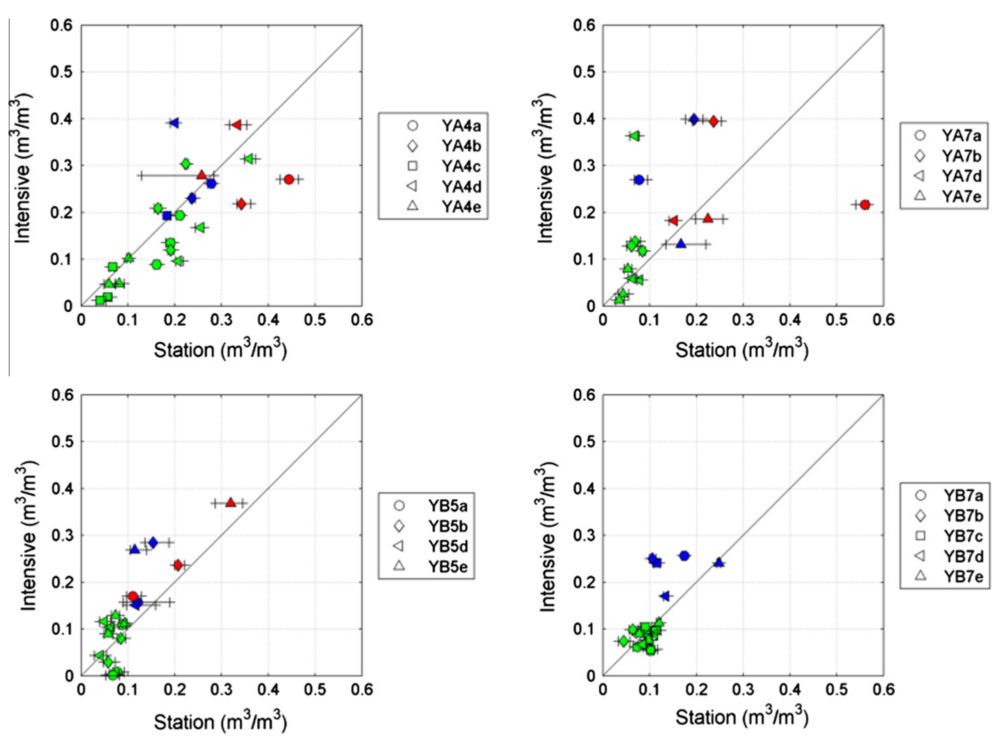

Fig. 5. Stations vs closest intensive sampling soil moisture for each focus area. Horizontal whiskers: daily variation of the station. The intensive sampling points used to compare with the daily average from the stations are nodes closest to the station. Blue: SMAPEx-1, Red: SMAPEx-2, Green: SMAPEx-3. (For interpretation of the references to color in this figure legend, the reader is referred to the web version of this article.)

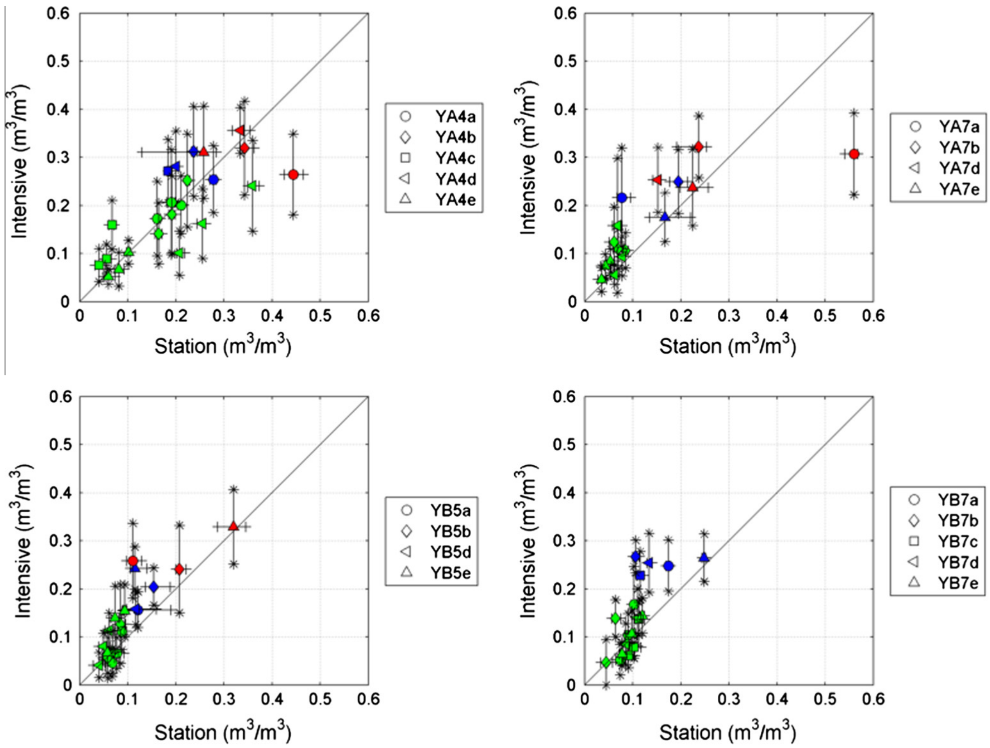

Fig. 6. Station vs intensive sampling soil moisture within 1 km for each focus area. Horizontal whiskers: daily variation of the station. Vertical whiskers: standard deviation of the intensive samples within the pixel. Blue: SMAPEx-1, Red: SMAPEx-2, Green: SMAPEx-3. (For interpretation of the references to color in this figure legend, the reader is referred to the web version of this article.)

to pixel comparisons, with dry biases of 0.04 m^3/m^3, whereas YB7e was representative of the YB7 3 km pixel, with an overall bias of 0.01 m^3/m^3. On average, all stations were drier than the average intensive measurements with biases ranging up to a maximum of 0.09 m^3/m^3 for YA4, 0.12 m^3/m^3 for YA7, 0.06 m^3/m^3 for YB5 and 0.08 m^3/m^3 for YB7. As all stations within these homogeneous pixels were relatively close to the spatial mean, a single station was found to be adequate for estimating areal average soil moisture of homogeneous areas; a result also found by Chen et al. (2014).

Intensive sampling is compared with the average of all stations within their respective 3 km pixels in Fig. 8. Daily variation of soil moisture from the stations show a large range, particularly during SMAPEx-2 due to high variability between stations, caused by the high spatial rather than temporal variability of soil moisture. Generally, the average of all stations compared well with the areal average from intensive sampling (e.g. YA4 3 km pixel). The average biases were 0.07 m^3/m^3 within YA4 and YA7 3 km pixels, 0.05 m^3/m^3 within YB5, and 0.03 m^3/m^3 for stations within the YB7 3 km pixel. However, it can be seen that by using a representative station (e.g. YA4a, YA7b, YB5e and YB7e based on Fig. 7) instead of the average of all the stations (Fig. 8), better agreement can be found between the representative stations and the average of all intensive samples.

The bias between YA7b and the average of the intensive samples was 0.04 m^3/m^3 whereas the bias between the average of all stations compared to intensive sampling was 0.12 m^3/m^3. Recall that YA7a was previously found to highly overestimate soil moisture (Fig. 6). However, by including measurements from YA7a when averaging all stations for YA7, comparisons with intensive measurements moved closer to the 1:1 line. If YA7a was eliminated, the bias between intensive samples and station averages would be greater. This reiterates the importance of understanding the spatial representativeness of each station for satellite validation.

Another observation is that representative stations identified based on the average of the intensive measurements were different from those identified in the previous section based on temporal stability analysis (Table 2). In fact, YB7e, which had almost no bias compared to intensive measurements was found to be the least representative based on the temporal stability analysis (Fig. 2). Likewise, YB5e and YA7b were not representative based on the temporal stability analysis regardless of the indicator used to determine representativeness. However, as shown from doing the temporal stability analysis with and without eliminating stations from one scale to another, replacing these stations into the temporal stability analysis is unlikely to have a large effect at 9 km and 36 km scales. In addition, intensive measurements (Fig. 7) showed that stations within the YB7 3 km pixel were generally drier than intensive measurements with the exception of YB7e. This was also observed in Figs. 5, 6 and 8 whereby station measurements were mostly lower than the intensive measurements.

Heathman et al. (2012) also found that permanent sensors tend to be biased, and that they varied more than areal average soil moisture conditions. While it is difficult to identify the cause, site installation and/or maintenance activities might increase disturbance around the immediate surroundings of the station. Cattle are also drawn towards these stations, thereby further increasing disturbance to the surroundings. This makes it difficult for vegetation to establish itself around the station and leads to bare ground surfaces, which leads to an increase in soil evaporation. If this was the case, it may explain the reason why YA7b, YB5e and YB7e were found to be the least representative stations based on the temporal stability analysis when the opposite may be true.

Finally, for the 36 km pixel, the station measurements were compared with the average of data retrieved from airborne observation. Based on this comparison, it was found that YB7e was the most representative followed by YA5, with overall biases of 0.009 m^3/m^3 and 0.010 m^3/m^3 respectively. However, since there were only 9 days of airborne soil moisture observations during the Austral spring, any conclusions on the representative stations need to be tempered by this fact. While YB7e agrees well with

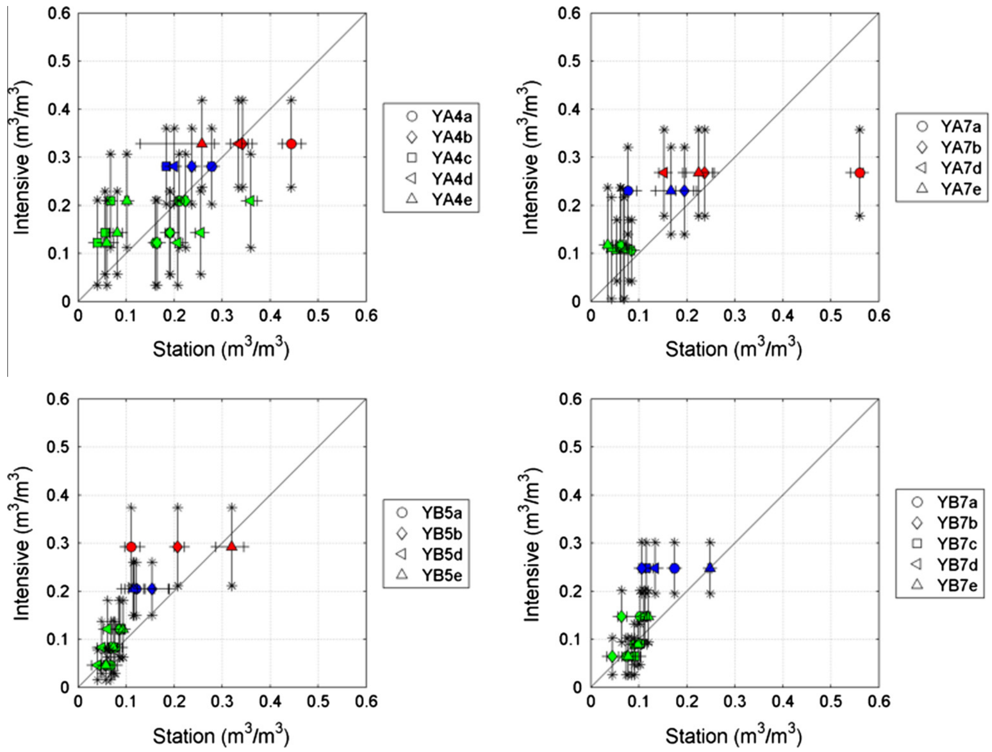

Fig. 7. Individual station vs intensive sampling soil moisture within 3 km for each focus area. Horizontal whiskers: daily variation of the station. Vertical whiskers: standard deviation of the intensive samples within the pixel. Blue: SMAPEx-1, Red: SMAPEx-2, Green: SMAPEx-3. (For interpretation of the references to color in this figure legend, the reader is referred to the web version of this article.)

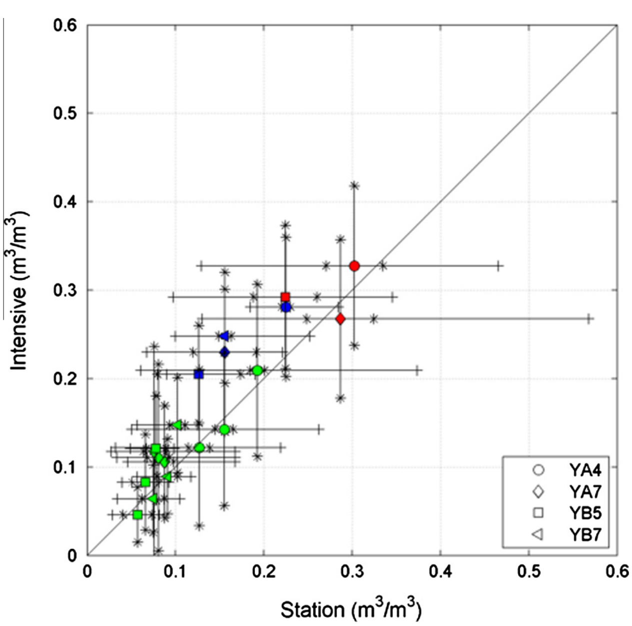

Fig. 8. Average of all stations vs intensive sampling soil moisture within 3 km. Horizontal whiskers: daily variation based on all stations within the focus area. Vertical whiskers: standard deviation of the intensive samples within the 3 km pixel. Blue: SMAPEx-1, Red: SMAPEx-2, Green: SMAPEx-3. (For interpretation of the references to color in this figure legend, the reader is referred to the web version of this article.)

the areal average during the campaign, it does not appear to be representative for periods outside the campaign (Fig. 4; bottom panel). Nevertheless, despite being only based on 9 days of airborne soil moisture product, this analysis identifies YA5 as a station that agrees best with the aircraft soil moisture with and overall bias of 0.010 m^3/m^3, followed by Y7 and Y5 (overall biases of 0.014 m^3/m^3 and 0.015 m^3/m^3 respectively) which were also identified based on a temporal stability analysis. Similarly, based on 11 days of airborne soil moisture derived from the National Airborne Field Experiment (NAFE), Azcurra and Walker (2009) identified Y5, Y7, Y10 and Y12 to be representative of Yanco's areal average soil moisture within an accuracy of 0.04 m^3/m^3.

5.3. Geostatistical analysis

5.3.1. Variograms

Standard variograms were derived for each 3 km pixel based on intensive samples. The range and sill derived from fitting the Whittle model to the experimental standard variograms are plotted as the black line in Fig. 9. Fitting variograms to observations within YA4 and YA7 was less accurate due to the presence of mixed land use. Nuggets derived from the model fitting were mostly 0 or close to, which indicates that measurement errors and variation within distances smaller than the sampling interval (250 m) were small. Referring to comparisons between stations and closest intensive samples, the underestimation by stations compared to intensive samples were larger than these nuggets, and the observed constant offset may therefore be related to disturbance around the immediate surroundings of the station as discussed previously, rather than measurement errors or small scale variability.

A positive relationship between range and sill with mean soil moisture can be observed for pixels within the YB area as in De Lannoy et al. (2006). Conversely, although the sill for both YB5 and YB7 were well defined, this was not the case for YA4 and YA7. In fact, YA4 showed multi-scale nested variograms which changed across campaigns (not shown here). However, of these nested variograms, one with the shortest range (<0.5 km) was consistently the same for all seasons and was similar to that of the other 3 km pixels. This consistent correlation length is likely

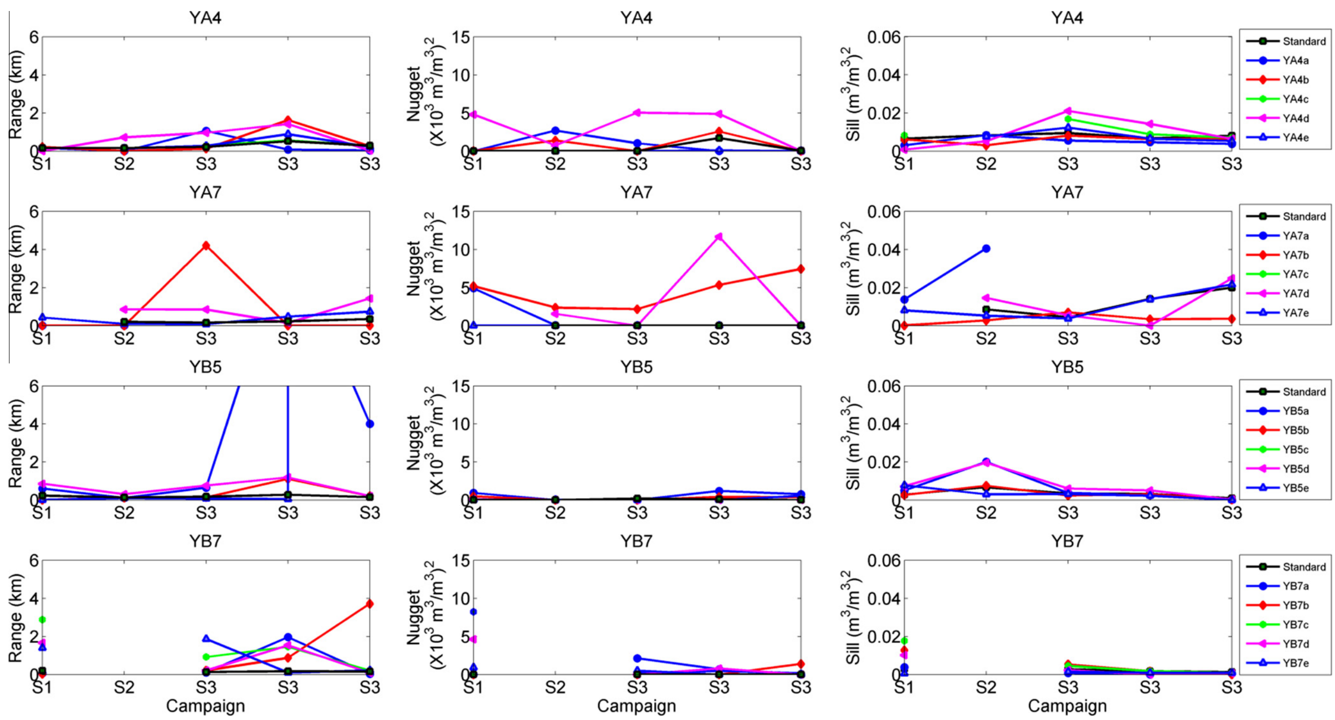

Fig. 9. Timeseries of parameters derived from fitting the Whittle model to the standard and centered-variogram of all stations based on intensive measurements for each 3 km pixel. S1: SMAPEx-1; S2: SMAPEx-2; S3: SMAPEx-3.

caused by land surface features which remain constant, or which vary slowly, such as vegetation and soil texture (Ryu and Famiglietti, 2006). Longer correlation lengths or ranges are likely to coincide with the sizes of fields. Compared to YA4, the presence of multi-scale variograms was less pronounced as variability within YA7 was lower. For instance, during SMAPEx-3, wheat and bare soil planted with corn could be found in YA7, whereas wheat, barley, linseed, bare soil and pasture could be found within the YA4 pixel. Based on these variograms, agricultural activities within the YA4 pixels clearly had a large influence on the spatial variability of soil moisture within the 3 km pixels.

As with the intensive samples, standard variograms were also derived for the 36 km pixel based on airborne soil moisture. Time-series of the range, nugget and sill derived for the standard variograms (black line in Fig. 10, left panels) correlated well with the wetting and drying cycles during the campaign. From the 5th to the 7th of September 2011, 5 mm of rain was recorded at the site, and from the 10th to the 12th another 3 mm of rain fell. After rainfall events, the derived variogram parameters changed and would decrease during the dry-down period. While the change in nugget and sill were correlated to each other, this relationship was less clear in the case of range. The change of correlation length has been observed in many previous studies, but the dependency of correlation length with soil moisture status is still inconclusive (Vereecken et al., 2014). The experimental standard variograms for each day of flight are also plotted in Fig. 10 (right panels). Note that the variogram is the same for all three right panels in Fig. 10 as it is derived from the same 36 km pixel. Based on the standard variograms for each day, the geostatistical structure of the 36 km pixel is seen to evolve with soil moisture conditions as also observed by Western et al. (1998) for the Tarrawarra catchment. Compared to 3 km pixels, at 36 km, the effect of anthropogenic activities (~1 km) on soil moisture variation diminishes as the influence of soil and vegetation properties and precipitation takes over (~10–30 km) (Ryu and Famiglietti, 2006).

5.3.2. Centered-variogram

In the case of the centered-variograms, due to the high variability of soil moisture within close distances (250 m spacing), the goodness of fit between the experimental centered-variograms and its fitted models were low for intensive measurements (R^2 ranged from 0.08 to 0.49). Fig. 9 shows how the parameters for the centered-variograms evolved during separate campaigns (different colors for each 3 km pixel) in comparison to that of the standard variogram (black). Differences between stations were smaller for YB7 compared to the other 3 km pixels. Some stations displayed the same dynamics as that of the standard variograms whereas others showed the opposite. Due to the poor fit of the models and edge-effects due to location of stations close to edges of the sampling grid, not much could be deduced from these parameters. Nevertheless, based on the correlation of parameters derived from the standard and centered-variograms, YA4e, YA7e, YB5d and YB7a would have been identified as representative stations of their respective 3 km pixels. The results were not consistent with any of the other identification methods. As the derived range based on standard variograms was 0.5 km and approximately 3 km based on centered-variograms, it is recommended for future studies seeking to apply the centered-variogram to extend intensive sampling at least 3 km away from the station with sampling intervals of less than 500 m to prevent edge-effects.

In the case of airborne soil moisture, the standard variogram models were on average able to explain more than 70% of the variability of the experimental centered-variogram derived from the airborne soil moisture product, a huge improvement compared to R^2 of intensive measurements due to the increase in sampling scale. Parameters derived from fitting the experimental centered-variograms are compared to the standard variogram in Fig. 10. Changes in the derived parameters correspond to rainfall events. By comparing the correlation between the derived parameters from standard and centered-variograms based on airborne soil moisture, multiple stations were found to exhibit similar spatial

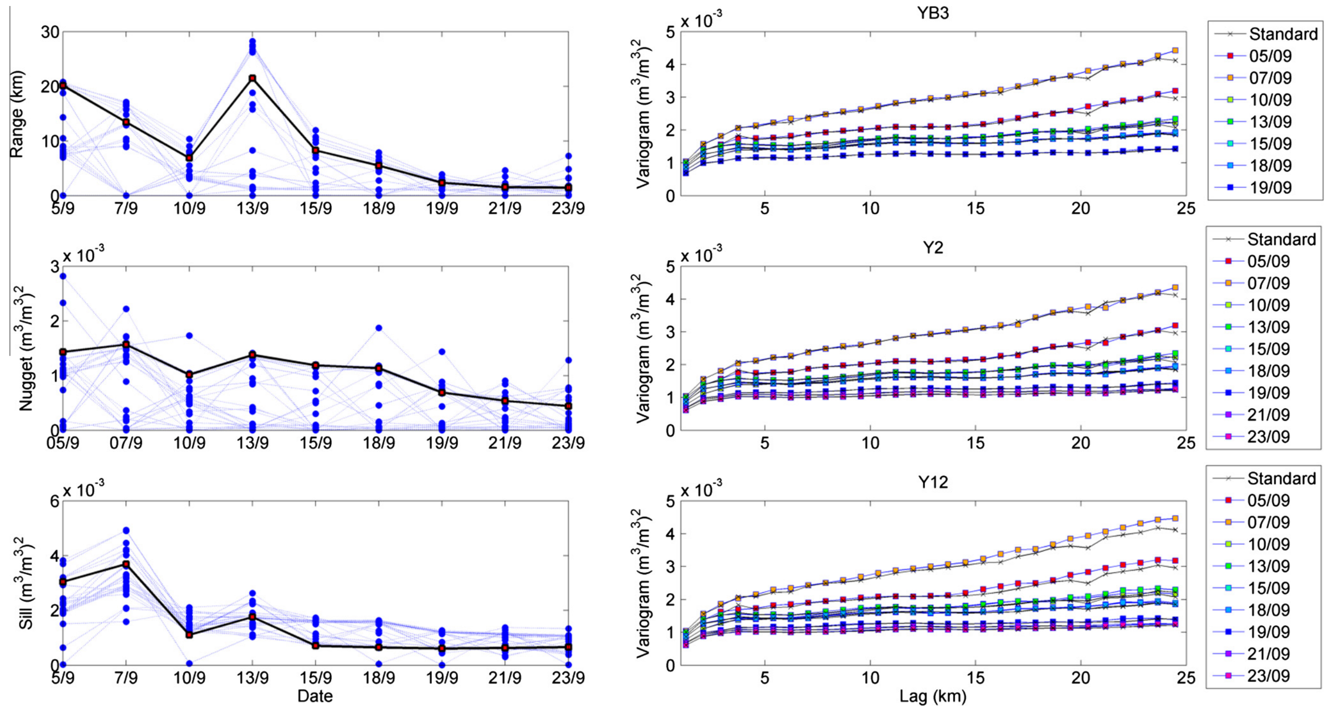

Fig. 10. Left panels: Timeseries of parameters derived from fitting the Whittle model to the standard (black) and centered-variogram (blue) of all stations based on airborne derived soil moisture. Right panels: Comparison of experimental variograms derived from standard variograms and centered-variogram of representative stations (YB3, Y2 and Y12) for different days. (For interpretation of the references to color in this figure legend, the reader is referred to the web version of this article.)

structures at 36 km. Correlation between models derived from standard and centered-variogram of stations ranged from 0.19 to 1.00 with an average of 0.70 whereas RMSE was between 0.002 $(m^3/m^3)^2$ and 0.054 $(m^3/m^3)^2$ with an average of 0.008 $(m^3/m^3)^2$. This shows that the majority of the stations within the network were able to capture the rainfall events during SMAPEx-3. YB3, Y2 and Y12 were found to perform the best and the experimental centered-variograms from these stations are shown in Fig. 10 (right panels).

5.4. Recommendations

Table 2 summarizes the representative stations identified based on different indicators from the temporal stability analysis, point to pixel comparisons using intensive ground measurements or airborne soil moisture products, and the centered-variogram analysis. Representative stations identified based on the different methods, or by using the average of all stations, were generally able to capture the rainfall events from January 2013 to December 2014 (Fig. 4, bottom panel). Based on the results and observations in this study, land use and soil and vegetation properties play an important role at local (3 km and 9 km) scales whereas rainfall patterns are expected to be more crucial at regional (36 km) scales. While the study site contained a mix of landuse/cover, it is to be noted that the effects of topography on soil moisture variability were not considered as the region has little relief, typical of most Australian landscapes. Considering this, the following recommendations are made.

1. Where intensive measurements are available, stations which are most representative of the areal mean should be used (Cosh, 2004). Stations YB5e and YB7e, with an estimated error of 0.03 m^3/m^3 and 0.01 m^3/m^3, respectively, are recommended for validating 3 km SMAP products within the YB area.
2. In the presence of agricultural activities, stations which are most representative of the areal average rather than the most ranked stable station should be used. Stations YA4b and YA7b, with estimated errors of 0.04 m^3/m^3, should be used for validating SMAP 3 km products within the YA area.
3. As decisions made by farmers are difficult to predict and affects the rank-stability of the stations, temporal stability analysis is not recommended in the presence of cropping activities. Instead, a good distribution of stations to account for variability within the pixel is important. A weighting method based on sizes of agricultural fields can then be applied.
4. Where intensive measurements are not available and the difference in MRD between stations are small, temporal stability analysis is adequate providing that stations are well distributed within the area of interest and the appropriate performance indicator selected, i.e. $RMSE_s$.
5. As the stations are well distributed in the Yanco study area, YA5 and YB7a, identified based on temporal stability methods, are likely to provide a good measure of the areal average of 9 km SMAP products.
6. Spatial average soil moisture based on airborne measurements, can be used for identifying representative stations at the 36 km scale, such as YA5. Other datasets such as the 1 km soil moisture product based on the ENVISAT ASAR Global Mode (Doubkova et al., 2009) and Sentinel-1 (Wagner et al., 2009) can possibly be used in the same way as the airborne data if of sufficient quality.
7. The results based on the centered-variogram analysis are biased due to edge-effects and are therefore non-conclusive. Consequently, it is recommended that this analysis to be repeated with observations extending at least 5 km from all stations for low resolution products and 500 m for higher resolution products (e.g. 3 km and 9 km) before the utility of centered-variograms can be verified.

8. Should resources become limited, priority should be given to maintain representative stations shown in Table 2.

6. Conclusion

Validation of satellite soil moisture products is faced with difficulties due to differences in scales between point measurements and satellite products. The ability to represent a mean temporal pattern and the areal average soil moisture is important in the validation of satellite soil moisture products. Therefore, this study sought to investigate the representativeness of soil moisture stations within the study area based on both temporal and spatial statistical methods.

Comparisons carried out with long-term soil moisture records and a limited set of intensive measurements revealed that stations identified as representative based on temporal stability analysis are not necessarily representative of the areal average soil moisture. Moreover, rank or time stable locations have a tendency to favor dry-biased stations. In addition, site installation and management activities may lead to biases in the station measurements. Therefore, where intensive measurements are available, they should be used to identify the most representative station. However, as intensive measurements are not always available, temporal stability was shown to be useful provided that the stations are well-distributed across the area of interest. But for an area where mixed land use is present, a weighting method was recommended.

As stations within the Yanco study area were well distributed within different land use types, OzNet was shown to be useful in providing areal average soil moisture measurements for long-term validation and calibration of satellite soil moisture products and hydrological models. Based on available resources, representative stations or methods to estimate the areal average soil moisture for each SMAP pixel were also recommended in Table 2. Finally, airborne soil moisture products have been shown to be useful as *a priori* information for identifying representative locations based on point-to-pixel comparisons whereas further investigation is needed for the centered-variogram analysis.

Acknowledgments

This study was made possible through the provision of SMAPEx and OzNet data financially supported by grants from the Australian Research Council (ARC). MS Yee acknowledges the support from the Australian Postgraduate Award (APA) Scholarship. We would also like to thank Frank Winston and Rodger Young who provided valuable contributions in the installation and maintenance of the soil moisture stations. Thanks also to all the SMAPEx 1–3 experiment participants.

References

Albergel, C., de Rosnay, P., Gruhier, C., Muñoz-Sabater, J., Hasenauer, S., Isaksen, L., Kerr, Y., Wagner, W., 2012. Evaluation of remotely sensed and modelled soil moisture products using global ground-based in situ observations. Remote Sens. Environ. 118 (March), 215–226.

Azcurra, C., Walker, J.P., 2009. Towards SMOS validation in south-eastern Australia. In: 18th World IMACS Congress and MODSIM09 International Congress on Modelling and Simulation. Modelling and Simulation Society of Australia and New Zealand and International Association for Mathematics and Computers in Simulation, pp. 3675–3681.

Bittelli, M., 2011. Measuring soil water content: a review. HortTechnology 21 (3), 293–300.

Bosch, D.D., Lakshmi, V., Jackson, T.J., Choi, M., Jacobs, J.M., 2006. Large scale measurements of soil moisture for validation of remotely sensed data: Georgia soil moisture experiment of 2003. J. Hydrol. 323 (1), 120–137.

Brocca, L., Tullo, T., Melone, F., Moramarco, T., Morbidelli, R., 2012. Catchment scale soil moisture spatial–temporal variability. J. Hydrol. 422–423, 63–75.

Chen, M., Willgoose, G.R., Saco, P.M., 2014. Spatial prediction of temporal soil moisture dynamics using HYDRUS-1D. Hydrol. Process. 28 (2), 171–185.

Choi, M., Jacobs, J.M., Bosch, D.D., 2008. Remote sensing observatory validation of surface soil moisture using Advanced Microwave Scanning Radiometer E, Common Land Model, and ground based data: case study in SMEX03 Little River Region, Georgia. U.S. Water Resour. Res. 44 (8), W08421.

Cosh, M.H., 2004. Watershed scale temporal and spatial stability of soil moisture and its role in validating satellite estimates. Remote Sens. Environ. 92 (4), 427–435.

Cosh, M.H., Jackson, T.J., Starks, P., Heathman, G., 2006. Temporal stability of surface soil moisture in the Little Washita River watershed and its applications in satellite soil moisture product validation. J. Hydrol. 323 (1–4), 168–177.

Crow, W.T., Berg, A.A., Cosh, M.H., Loew, A., Mohanty, B.P., Panciera, R., de Rosnay, P., Ryu, D., Walker, J.P., 2012. Upscaling sparse ground-based soil moisture observations for the validation of coarse-resolution satellite soil moisture products. Rev. Geophys. 50 (2), RG2002.

Crow, W.T., Ryu, D., Famiglietti, J.S., 2005. Upscaling of field-scale soil moisture measurements using distributed land surface modeling. Adv. Water Resour. 28 (1), 1–14.

De Lannoy, G.J.M., Verhoest, N.E.C., Houser, P.R., Gish, T.J., Van Meirvenne, M., 2006. Spatial and temporal characteristics of soil moisture in an intensively monitored agricultural field (OPE 3). J. Hydrol. 331 (3–4), 719–730.

de Wit, A., van Diepen, C., 2007. Crop model data assimilation with the Ensemble Kalman filter for improving regional crop yield forecasts. Agric. For. Meteorol. 146 (1–2), 38–56.

Delworth, T.L., Manabe, S., 1988. The influence of potential evaporation on the variabilities of simulated soil wetness and climate. J. Clim. 1 (5), 523–547.

Disseldorp, D., Yee, M., Monerris, A., Walker, J., 2013. A temporal stability analysis of the Australian SMAP mission validation site. In: Boland, J., Piantadosi, J. (Eds.), 20th International Congress on Modelling and Simulation. Modelling and Simulation Society of Australia and New Zealand, Adelaide, pp. 2869–2875.

Dorigo, W.A., Wagner, W., Hohensinn, R., Hahn, S., Paulik, C., Xaver, A., Gruber, A., Drusch, M., Mecklenburg, S., van Oevelen, P., Robock, A., Jackson, T., 2011. The international soil moisture network: a data hosting facility for global in situ soil moisture measurements. Hydrol. Earth Syst. Sci. 15 (5), 1675–1698.

Doubkova, M., Bartsch, A., Pathe, C., Sabel, D., Wagner, W., 2009. The medium resolution soil moisture dataset: overview of the SHARE ESA DUE TIGER project. 2009 IEEE International Geoscience and Remote Sensing Symposium, vol. 1. IEEE, pp. I-116–I-119.

Draper, C.S., Walker, J.P., Steinle, P.J., de Jeu, R.A.M., Holmes, T.R.H., 2009. An evaluation of AMSR-E derived soil moisture over Australia. Remote Sens. Environ. 113 (4), 703–710.

Engman, E.T., 1991. Applications of microwave remote sensing of soil moisture for water resources and agriculture. Remote Sens. Environ. 35 (2–3), 213–226.

Entekhabi, D., Reichle, R.H., Koster, R.D., Crow, W.T., 2010. Performance metrics for soil moisture retrievals and application requirements. J. Hydrometeorol. 11 (3), 832–840.

Famiglietti, J.S., Devereaux, J.A., Laymon, C.A., Tsegaye, T., Houser, P.R., Jackson, T.J., Graham, S.T., Rodell, M., van Oevelen, P.J., 1999. Ground-based investigation of soil moisture variability within remote sensing footprints During the Southern Great Plains 1997 (SGP97) Hydrology Experiment. Water Resour. Res. 35 (6), 1839–1851.

Famiglietti, J.S., Ryu, D., Berg, A.A., Rodell, M., Jackson, T.J., 2008. Field observations of soil moisture variability across scales. Water Resour. Res. 44 (1), W01423.

Gao, X., Wu, P., Zhao, X., Wang, J., Shi, Y., Zhang, B., Tian, L., Li, H., 2013. Estimation of spatial soil moisture averages in a large gully of the Loess Plateau of China through statistical and modeling solutions. J. Hydrol. 486 (April), 466–478.

Gómez-Plaza, A., Alvarez-Rogel, J., Albaladejo, J., Castillo, V.M., 2000. Spatial patterns and temporal stability of soil moisture across a range of scales in a semi-arid environment. Hydrol. Process. 14 (7), 1261–1277.

Grayson, R.B., Western, A.W., 1998. Towards areal estimation of soil water content from point measurements: time and space stability of mean response. J. Hydrol. 207 (1–2), 68–82.

Gruber, A., Dorigo, W., Zwieback, S., Xaver, A., Wagner, W., 2013. Characterizing coarse-scale representativeness of in situ soil moisture measurements from the international soil moisture network. Vadose Zone J. 12 (2).

Heathman, G.C., Cosh, M.H., Han, E., Jackson, T.J., McKee, L., McAfee, S., 2012. Field scale spatiotemporal analysis of surface soil moisture for evaluating point-scale in situ networks. Geoderma 170, 195–205.

Hu, W., Tallon, L.K., Si, B.C., 2012. Evaluation of time stability indices for soil water storage upscaling. J. Hydrol. 475, 229–241.

Jackson, T., Schmugge, T., O'Neill, P., 1984. Passive microwave remote sensing of soil moisture from an aircraft platform. Remote Sens. Environ. 14 (1–3), 135–151.

Jackson, T.J., Cosh, M.H., Bindlish, R., Starks, P.J., Bosch, D.D., Seyfried, M., Goodrich, D.C., Moran, M.S., Du, J., 2010. Validation of advanced microwave scanning radiometer soil moisture products. IEEE Trans. Geosci. Remote Sens. 48 (12), 4256–4272.

Jackson, T.J., Le Vine, D.M., Hsu, A.Y., Oldak, A., Starks, P.J., Swift, C.T., Isham, J.D., Haken, M., 1999. Soil moisture mapping at regional scales using microwave radiometry: the Southern Great Plains Hydrology Experiment. IEEE Trans. Geosci. Remote Sens. 37 (5), 2136–2151.

Jacobs, J.M., Mohanty, B.P., Hsu, E.-C., Miller, D., 2004. SMEX02: field scale variability, time stability and similarity of soil moisture. Remote Sens. Environ. 92 (4), 436–446.

Janis, M.J., Robeson, S.M., 2004. Determining the spatial representativeness of air-temperature records using variogram-nugget time series. Phys. Geogr. 25 (6), 513–530.

Joshi, C., Mohanty, B.P., 2010. Physical controls of near-surface soil moisture across varying spatial scales in an agricultural landscape during SMEX02. Water Resour. Res. 46 (12), W12503.

Kerr, Y., Waldteufel, P., Wigneron, J.-P., Delwart, S., Cabot, F., Boutin, J., Escorihuela, M.-J., Font, J., Reul, N., Gruhier, C., Juglea, S., Drinkwater, M., Hahne, A., Martin-Neira, M., Mecklenburg, S., 2010. The SMOS mission: new tool for monitoring key elements of the global water cycle. Proc. IEEE 98 (5), 666–687.
Koster, R.D., 2004. Regions of strong coupling between soil moisture and precipitation. Science 305, 1138–1140.
Koster, R.D., Guo, Z., Yang, R., Dirmeyer, P.A., Mitchell, K., Puma, M.J., 2009. On the nature of soil moisture in land surface models. J. Clim. 22 (16), 4322–4335.
Li, D., Shao, M., 2015. Temporal stability of soil water storage in three landscapes in the middle reaches of the Heihe River, northwestern China. Environ. Earth Sci. 73 (7), 3095–3107.
Martínez, G., Pachepsky, Y.A., Vereecken, H., 2014. Temporal stability of soil water content as affected by climate and soil hydraulic properties: a simulation study. Hydrol. Process. 28 (4), 1899–1915.
Martínez-Fernández, J., Ceballos, A., 2003. Temporal stability of soil moisture in a large-field experiment in Spain. Soil Sci. Soc. Am. J. 67 (6), 1647–1656.
Martínez-Fernández, J., Ceballos, A., 2005. Mean soil moisture estimation using temporal stability analysis. J. Hydrol. 312 (1–4), 28–38.
McNairn, H., Jackson, T.J., Wiseman, G., Belair, S., Berg, A., Bullock, P., Colliander, A., Cosh, M.H., Kim, S.-B., Magagi, R., Moghaddam, M., Njoku, E.G., Adams, J.R., Homayouni, S., Ojo, E., Rowlandson, T., Shang, J., Goita, K., Hosseini, M., 2015. The soil moisture active passive validation experiment 2012 (SMAPVEX12): prelaunch calibration and validation of the SMAP soil moisture algorithms. IEEE Trans. Geosci. Remote Sens. 53 (5), 2784–2801.
Merlin, O., Walker, J.P., Kalma, J.D., Kim, E.J., Hacker, J., Panciera, R., Young, R., Summerell, G., Hornbuckle, J., Hafeez, M., Jackson, T., 2008. The NAFE06 data set: towards soil moisture retrieval at intermediate resolution. Adv. Water Resour. 31 (11), 1444–1455.
Merlin, O., Walker, J.P., Panciera, R., Young, R., Kalma, J.D., Kim, E.J., 2007. Soil moisture measurement in heterogeneous terrain. In: Modsim 2007: International Congress on Modelling and Simulation, pp. 2604–2610.
Mohanty, B.P., Skaggs, T.H., 2001. Spatio-temporal evolution and time-stable characteristics of soil moisture within remote sensing footprints with varying soil, slope, and vegetation. Adv. Water Resour. 24 (9–10), 1051–1067.
Pal, J.S., Eltahir, E.A.B., 2003. A feedback mechanism between soil-moisture distribution and storm tracks. Quart. J. Roy. Meteorol. Soc. 129 (592), 2279–2297.
Panciera, R., Walker, J.P., Jackson, T.J., Gray, D.A., Tanase, M.A., Ryu, D., Monerris, A., Yardley, H., Rüdiger, C., Wu, X., Gao, Y., Hacker, J.M., 2014. The soil moisture active passive experiments (SMAPEx): toward soil moisture retrieval from the SMAP mission. IEEE Trans. Geosci. Remote Sens. 52 (1), 490–507.
Peischl, S., Walker, J.P., Rüdiger, C., Ye, N., Kerr, Y.H., Kim, E., Bandara, R., Allahmoradi, M., 2012. The AACES field experiments: SMOS calibration and validation across the Murrumbidgee River catchment. Hydrol. Earth Syst. Sci. 16, 1697–1708.
Penna, D., Brocca, L., Borga, M., Dalla Fontana, G., 2013. Soil moisture temporal stability at different depths on two alpine hillslopes during wet and dry periods. J. Hydrol. 477 (January), 55–71.
Prigent, C., Aires, F., Rossow, W.B., Robock, A., 2005. Sensitivity of satellite microwave and infrared observations to soil moisture at a global scale: relationship of satellite observations to in situ soil moisture measurements. J. Geophys. Res.: Atmos. 110 (D7), D07110.
Qin, J., Yang, K., Lu, N., Chen, Y., Zhao, L., Han, M., 2013. Spatial upscaling of in-situ soil moisture measurements based on MODIS-derived apparent thermal inertia. Remote Sens. Environ. 138, 1–9.
Refsgaard, J.C., 1997. Parameterisation, calibration and validation of distributed hydrological models. J. Hydrol. 198 (1–4), 69–97.
Robock, A., Vinnikov, K.Y., Srinivasan, G., Entin, J.K., Hollinger, S.E., Speranskaya, N. A., Liu, S., Namkhai, A., 2000. The global soil moisture data bank. Bull. Am. Meteorol. Soc. 81 (6), 1281–1299.
Román, M.O., Schaaf, C.B., Woodcock, C.E., Strahler, A.H., Yang, X., Braswell, R.H., Curtis, P.S., Davis, K.J., Dragoni, D., Goulden, M.L., 2009. The MODIS (Collection V005) BRDF/albedo product: assessment of spatial representativeness over forested landscapes. Remote Sens. Environ. 113 (11), 2476–2498.
Rüdiger, C., Calvet, J.-C., Gruhier, C., Holmes, T.R.H., de Jeu, R.A.M., Wagner, W., 2009. An intercomparison of ERS-Scat and AMSR-E soil moisture observations with model simulations over France. J. Hydrometeorol. 10 (2), 431–447.
Ryu, D., Famiglietti, J.S., 2006. Multi-scale spatial correlation and scaling behavior of surface soil moisture. Geophys. Res. Lett. 33 (8), L08404.
Schneider, K., Huisman, J.A., Breuer, L., Zhao, Y., Frede, H.-G., 2008. Temporal stability of soil moisture in various semi-arid steppe ecosystems and its application in remote sensing. J. Hydrol. 359 (1–2), 16–29.
Smith, A.B., Walker, J.P., Western, A.W., Young, R.I., Ellett, K.M., Pipunic, R.C., Grayson, R.B., Siriwardena, L., Chiew, F.H.S., Richter, H., 2012. The Murrumbidgee soil moisture monitoring network data set. Water Resour. Res. 48 (7), W07701.
Vachaud, G., de Silans, A., Balabanis, P., Vauclin, M., 1985. Temporal stability of spatially measured soil water probability density function. Soil Sci. Soc. Am. J. 49 (4), 822–828.
Vanderlinden, K., Vereecken, H., Hardelauf, H., Herbst, M., Martínez, G., Cosh, M.H., Pachepsky, Y.A., 2012. Temporal stability of soil water contents: a review of data and analyses. Vadose Zone J. 11 (4).
Vereecken, H., Huisman, J., Pachepsky, Y., Montzka, C., van der Kruk, J., Bogena, H., Weihermüller, L., Herbst, M., Martinez, G., Vanderborght, J., 2014. On the spatio-temporal dynamics of soil moisture at the field scale. J. Hydrol. 516 (August), 76–96.
Vinnikov, K.Y., Robock, A., Qiu, S., Entin, J.K., Owe, M., Choudhury, B.J., Hollinger, S.E., Njoku, E.G., 1999. Satellite remote sensing of soil moisture in Illinois, United States. J. Geophys. Res. 104 (D4), 4145–4168.
Wagner, W., Sabel, D., Doubkova, M., Bartsch, A., Pathe, C., 2009. The potential of Sentinel-1 for monitoring soil moisture with a high spatial resolution at global scale. In: Symposium of Earth Observation and Water Cycle Science.
Walker, J.P., Willgoose, G.R., Kalma, J.D., 2001. One-dimensional soil moisture profile retrieval by assimilation of near-surface observations: a comparison of retrieval algorithms. Adv. Water Resour. 24 (6), 631–650.
Western, A.W., Blöschl, G., Grayson, R.B., 1998. Geostatistical characterisation of soil moisture patterns in the Tarrawarra catchment. J. Hydrol. 205 (1–2), 20–37.
Whittle, P., 1954. On stationary processes in the plane. Biometrika 41 (3–4), 434–449.
You-Jun, C., 2006. Letter to the Editor on "rank stability or temporal stability". Soil Sci. Soc. Am. J. 70 (1), 306.
Zhao, Y., Peth, S., Wang, X.Y., Lin, H., Horn, R., 2010. Controls of surface soil moisture spatial patterns and their temporal stability in a semi-arid steppe. Hydrol. Process. 24 (18), 2507–2519.
Zhou, J., Fu, B., Gao, G., Lü, N., Lü, Y., Wang, S., 2015. Temporal stability of surface soil moisture of different vegetation types in the Loess Plateau of China. CATENA 128, 1–15.